Stiffness Optimal Modulation of a Variable Stiffness Energy Storage Hip Exoskeleton and Experiments on Its Assistance Effect

Bingshan Hu, Fengchen Liu, Ke Cheng, Wenming Chen, *Member, IEEE*, Xinying Shan, and Hongliu Yu

***Abstract*— Lower limb energy storage assisted exoskeletons realize walking assistance by using the energy stored by elastic elements during walking. Such exoskeletons are characterized by a small volume, light weight and low price. However, energy storage assisted exoskeletons adopt fixed stiffness joints typically, which cannot adapt to changes of the wearer's height, weight, or walking speed. In this study, based on the analysis of the energy flow characteristics and stiffness change characteristics of lower limb joints during a human walking on flat ground, a novel variable stiffness energy storage assisted hip exoskeleton is designed, and a stiffness optimization modulation method is proposed to store most of the negative work done by the human hip joint when walking. Through the analysis of the surface electromyography signals of the rectus femoris and long head of the biceps femoris, it is found that the muscle fatigue of the rectus femoris is reduced by 8.5% under the optimal stiffness assistance condition, and the exoskeleton provides better assistance under the optimal stiffness assistance condition.**

***Index Terms*— Energy storage, assisted exoskeleton, hip joint, optimal, stiffness modulation.**

I. Introduction

WALKING is the most common movement pattern in life. At present, many assistive devices have been developed all over the world to enhance walking ability. Walking for long periods of time will lead to muscle fatigue and reduced walking ability. Wearing an assisted exoskeleton can improve the wearer's walking ability significantly. According to the actuating mode, assisted exoskeletons can be divided into active assisted exoskeletons and energy storage assisted exoskeletons. An active assisted exoskeleton is driven by external energy, which can convert electric, pneumatic, hydraulic or other energy into mechanical movement [1]. Since the first lower limb exoskeleton Hardiman was developed in the 1960s [2], great progress has been made in the development of active assisted exoskeletons. The BLEEX [3] exoskeleton developed by Berkeley Bionics is driven by hydraulic pressure and motor. Its weight is 38kg, and the walking speed can reach 1.3m/s. The HAL [4] lower limb rehabilitation robot can predict the human motion intention and control the motor to drive the exoskeleton to assist the human body. Its own weight is 15kg, and its price is about fifty thousand dollars. The Rex [5] exoskeleton weighs 38kg, and it has rechargeable batteries. And each Rex device is customized for patients, but its price is at least thirty thousand dollars. EksoNR [6] is a lower limb exoskeleton for acquired brain injury. It is equipped with high-precision sensors, micro drive motors. Its price is about one hundred thousand dollars. Although active exoskeletons have realized many functions at present, its characteristics of relying on external power, large volume and high price have made its related research into a bottleneck.

Energy storage assisted exoskeletons uses elastic elements to recover the energy during walking to achieve assisted walking or weight support without external energy for driving [7]. For example, Collins et al. developed an energy storage assist ankle exoskeleton which includes a passive clutch, and a spring parallel to the calf muscle and tendon [8]. Experiments showed that the metabolism of healthy people walking with the exoskeleton was reduced by about 7.2%. Experiments on the ankle exoskeleton designed by Mooney showed that the average positive power of six wearers decreased by 0.033 W/kg when walking at a speed of 1.4 m/s [9]. Zhou et al. found that most energy storage assisted lower limb exoskeletons can only assist with a specific gait [10], and he developed an exoskeleton that can adapt to two gaits [11]. Nasiri et al. designed an energy storage assisted hip exoskeleton according to the metabolic changes of the human body during running [12]. In addition, some flexible energy storage assisted exoskeletons provide tension parallel to human muscles or tendons to make the direction of assist force close to the direction of

Manuscript received 23 July 2022; revised 20 December 2022; accepted 5 January 2023. Date of publication 19 January 2023; date of current version 6 February 2023. This work was supported in part by the National Key Research and Development Program of China under Grant 2020YFC2005800 and Grant 2020YFC2005804, in part by the Natural Science Foundation of Shanghai China under Grant 20ZR1437800, and in part by the Biomedical Science and Technology support project of Shanghai under Grant 22S31901400. *(Corresponding author: Hongliu Yu.)*

This work involved human subjects or animals in its research. The authors confirm that all human/animal subject research procedures and protocols are exempt from review board approval.

Bingshan Hu and Hongliu Yu are with the Institute of Rehabilitation Engineering and Technology, University of Shanghai for Science and Technology, Shanghai 200093, China, and also with the Shanghai Engineering Research Center of Assistive Devices, Shanghai 200093, China (e-mail: hubingshan@usst.edu.cn; yhl_usst@outlook.com).

Fengchen Liu and Ke Cheng are with the Institute of Rehabilitation Engineering and Technology, University of Shanghai for Science and Technology, Shanghai 200093, China (e-mail: 213332681@st.usst.edu.cn; 193832306@st.usst.edu.cn).

Wenming Chen is with the Academy for Engineering and Technology, Fudan University, Shanghai 200433, China (e-mail: chenwm@fudan.edu.cn).

Xinying Shan is with the Beijing Key Laboratory of Rehabilitation Technical Aids for Old-Age Disability, National Research Center for Rehabilitation Technical Aids, Beijing 100176, China (e-mail: shanxinying@nrcrta.cn).

This article has supplementary downloadable material available at https://doi.org/10.1109/TNSRE.2023.3236256, provided by the authors.

Digital Object Identifier 10.1109/TNSRE.2023.3236256

human muscles, to make the gait more natural [13]. Some energy storage assisted exoskeletons can also be adjusted according to the anatomical differences of different people [14]. Their actuating methods mainly include cable actuator [15], pneumatic muscle [16], and new intelligent material drive [17].

At present, most active assisted exoskeletons use rigid actuators. In order to achieve better human–robot interaction, the use of flexible actuators has become a development direction of assisted exoskeletons. Because energy storage assisted exoskeletons needs to store energy, flexible links must be introduced. Currently, the common flexible actuators include the series elastic actuator (SEA) and variable stiffness actuator (VSA) [18]. The stiffness of the SEA is determined and it cannot be changed. In contrast, the mechanical stiffness of a VSA can be adjusted by changing the physical properties, preload, or transmission ratio of elastic elements to achieve a personalized configuration [19]. For example, Li et al. designed a compact VSA for exoskeletons, and the stiffness of the actuator is changed by using different winding modes of steel cable between pulley blocks [20]. Baser designed a variable stiffness (VS) ankle exoskeleton based on the adjustable transmission ratio mechanism, which can effectively reduce the human–robot interaction force and track the given torque command at different frequencies [21]. The VS ankle exoskeleton designed by Kumar can adjust the stiffness of the exoskeleton in real time through extremum seeking control algorithm to adapt to different walking speeds [22]. The knee joint VS actuator designed by Cestari sets three stiffness states according to the ground stiffness and walking speed [23].

Among the existing lower limb assisted exoskeletons, active exoskeleton has a significant effect on human capacity enhancement because it has an active power source outside the body. It has also been widely studied and applied in military and other fields. However, due to the price and weight of active exoskeleton, there is still much work to be done in the promotion of home use [24]. Energy storage assisted exoskeletons have the characteristics of using the energy of the human body to achieve assistance, so they do not need additional actuators or complex control algorithms. Therefore, increasingly energy storage exoskeletons are used in endurance tasks such as walking and jogging because of their simplicity and lightness [25]. However, the stiffness of most energy storage exoskeletons is not adjustable, and a universal stiffness optimization modulation theory has not been proposed.

In this study, after analyzing the power flow of lower limb joints during walking, a design for a VS energy storage assisted hip exoskeleton (VS-ESAH exoskeleton) is proposed. The exoskeleton is based on the cam roller stiffness adjustment principle, and a motor is used to adjust the spring preload to adjust the hip joint stiffness actively. Based on the bipedal walking dynamic model, a method to optimize the stiffness of exoskeleton is proposed according to the wearer's height, weight and walking speed. The rest of this paper is organized as follows. In the second section, the power changes of lower limb joints and the equivalent stiffness of the hip joint are analyzed. In the third section, the seven-link dynamic model of human lower limbs was established, and the optimal stiffness of VS-ESAH exoskeleton was calculated with the goal of storing as much energy as possible in the negative work stage of the hip joint. The fourth section introduces the mechanism design method for the VS-ESAH exoskeleton, and verifies the stiffness adjustment performance through a static torque experiment. In the fifth section, assistance performance experiments are carried out.

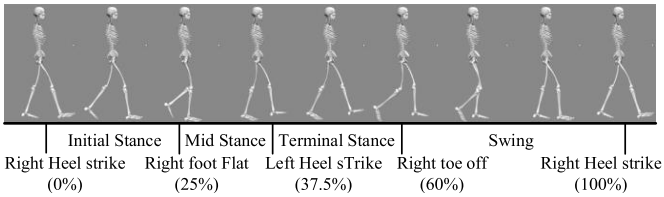

Fig. 1. Human gait cycle.

II. Analysis of Low Limb Joints Energy and Equivalent Stiffness During Walking

The selection of the assisted joint is an important problem in the design of exoskeletons. This section selects appropriate assisted joints based on analyzing the gait characteristics of human walking on the ground, and analyzes the changes of equivalent stiffness of hip joints during walking. As shown in Fig. 1, with the right foot following the ground as the starting position of the gait cycle, the support phase can be divided into three stages: the initial stance of the support phase is the process from the right heel striking the ground to the right foot being flat on the ground, which accounts for about 25% of the gait cycle. The mid stance of the support phase is the process from the right foot being flat on the ground to left heel striking the ground, which accounts for about 12.5% of the gait cycle. The terminal stance of the support phase is the process from the left heel striking the ground to the toe off of the right foot from the ground, which accounts for about 22.5% of the gait cycle.

A. Power Flow Characteristics of Lower Limb Joints

Using Gabriele Bovi's database [26], the changes of lower limb joint power in a gait cycle during walking are analyzed for the ankle joint, knee joint, and hip joint, and the results are shown in Fig. 2.

The elasticity of the tendon at the ankle joint is high, and the function of the tendon is similar to that of a spring, which can realize energy storage [27]. As shown in Fig. 2(a), the ankle joint does negative work in the initial stance and mid stance and positive work in the terminal stance. With the increase of walking speed, the time point of starting to do positive work will be relatively early, and the amplitude will increase significantly. The negative work area is approximately equal to the positive work area, indicating that the elastic element arranged at the ankle can store energy in the negative work area and be used for power assistance in the positive

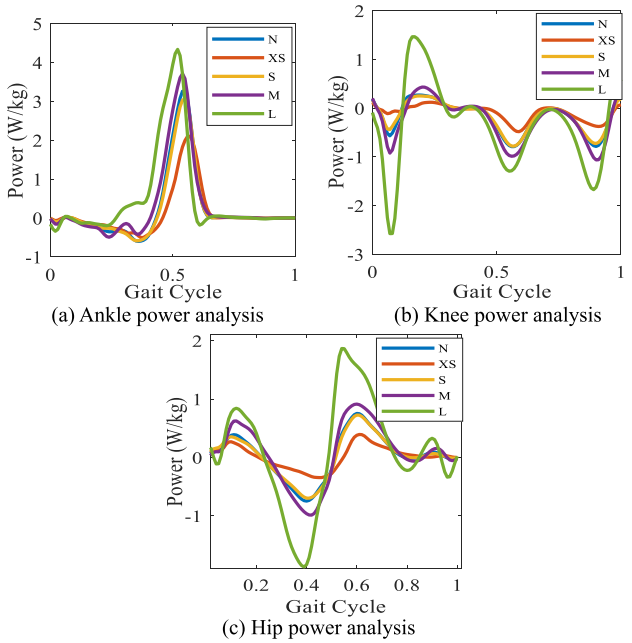

(a) Ankle power analysis (b) Knee power analysis

(c) Hip power analysis

Fig. 2. Power analysis of ankle, knee, and hip joints. According to the ratio of speed (V) to height (H), V/H, five walking states are identified, where N is the walking state with natural speed, XS is the walking state with V/H $<$ 0.6, S is the walking state with 0.6 $\leq$ V/H $\leq$ 0.8, M is the walking state with 0.8 $\leq$ V/H $\leq$ 1, and L is the walking state with V/H $>$ 1.

work area. However, the ankle joint is far away from the swing center of the lower limb. If the mass of the ankle exoskeleton is too large, it will be detrimental to walking metabolism, especially when the walking speed increases [28]. It can be seen from Fig. 2(b), when walking on flat ground, the knee joint only does some positive work in the mid stance, whereas it does negative work in the initial stance, terminal stance, and swing phase. If the knee joint is selected as the assisted joint, a large amount of energy will be released in a short positive work area, which will affect the stability of the knee joint. It means that the assisted range of the knee joint is short, so knee joint is not suitable as an assisted joint.

As shown in Fig. 2(c), the hip joint does positive work in the initial stance of the support phase, the first half of the mid stance of the support phase, and the first half of the swing phase. It does negative work in the second half of the mid stance of the support phase and the terminal stance of the support phase. Therefore, elastic elements can be added at the hip joint to store negative work and release it in the positive work stage to assist with thigh flexion so as to reduce the energy consumption during walking. In terms of work performance, both hip and ankle joints do a lot of positive work for exercise during walking, but hip muscle tissue consumes more energy than ankle muscle tissue when generating unit positive work [29]. Therefore, if elastic elements are used to store energy and assist hip, the efficiency of hip joint can be effectively improved. Moreover, the rotational motion of the hip around the coronal axis in the sagittal plane is the main actuating source in the walking process of the lower limbs. With the increase of age, some elderly people will gradually

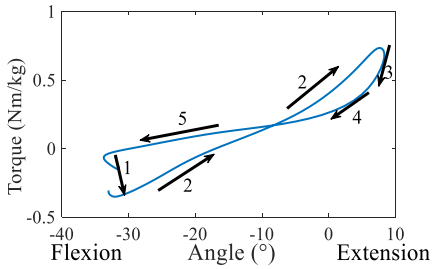

Fig. 3. Hip joint torque versus angle and equivalent stiffness in gait cycle.

increase their dependence on the hip during walking due to a fear of falling [30]. Therefore, we believe that compared with the ankle, which is far away from the rotation center of the lower limbs, assistance at the hip joint will be more conducive to reducing walking metabolism.

B. Equivalent Stiffness Analysis of the Hip Joint

According to Gabriele Bovi's data [26], the relationship between hip torque and rotation angle is shown in Fig. 3. The variation process of hip joint torque with angle is divided into five stages. Stage 1 is from the terminal stance of the swing phase to the initial stance of the support phase, stage 2 is in the support phase, stage 3 is from the terminal stance of the support phase to the initial stance of the swing phase, and stages 4 and 5 are in the swing phase. In the transition from stage 1 to stage 2, the hip torque will suddenly increase to the peak, which is caused by the heel strike. In the transition from stage 2 to stage 3, the torque of the hip joint increases gently, and the lower limbs transition from full foot landing to the maximum extension position. In the transition from stage 3 to stage 4, the torque of hip joint changes greatly. At this time, the lower limbs flex forward and are in the first half of the swing phase. In the transition from stage 4 to stage 5, the hip joint changes from the extension position to the flexion position, the torque changes gently, and the limbs are in the second half of the swing phase.

Through the previous analysis of the change of hip joint power and the torque with angle, it can be seen that in Fig. 3, the process of the hip joint doing negative work corresponds to process 2, and the process of doing positive work corresponds to process 3. In these two processes, the torque and angle of the hip joint show an approximate linear relationship, and the fitting slope is called the equivalent stiffness. Specifically, the data of each adjacent point in process 2 and process 3 are differentiated, divided by the corresponding change angle, and then the average value is calculated to obtain the equivalent stiffness. Fig. 4 shows the equivalent stiffness analysis of some subjects. Fig. 4(a) shows the equivalent stiffness of process 2 and process 3 when three people of different weights walk at 1 m/s, and Fig. 4(b) shows the equivalent stiffness of a person of 70 kg walking at different speeds. It can be seen that the equivalent stiffness of the human hip joint varies widely under different conditions. The equivalent stiffness of hip joint during flexion and extension changes under different height,

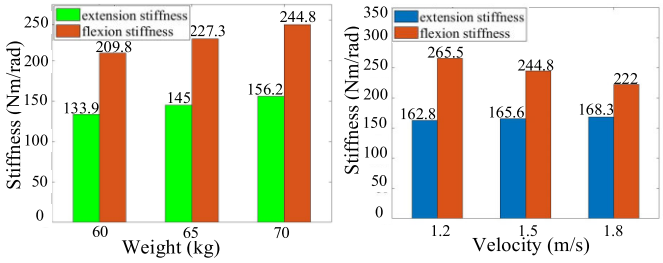

(a) Joint torque versus weight (b) Joint torque versus velocity

Fig. 4. Equivalent stiffness of hip joint under different conditions.

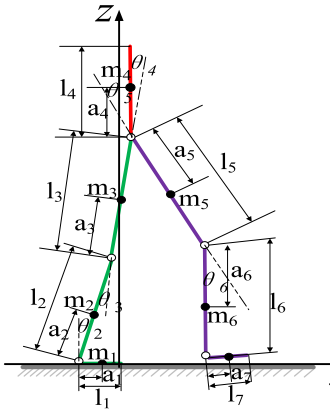

Fig. 5. Lower limb's seven link dynamic model.

weight and walking speed, this is also confirmed by previous studies.

III. Selection Method of the Optimal Assist Stiffness

The purpose of designing VS-ESAH exoskeleton is to enable the exoskeleton to make stiffness adjustments according to different individuals and different walking speeds. Therefore, it is necessary to optimize the stiffness of the VS joint. A novel stiffness optimization modulation method is proposed in this section, that is, to store as much negative work done by the hip joint during walking as possible in the elastic elements of the VS joint, so as to improve the assistance efficiency of the exoskeleton. Assuming that all negative work is stored as the elastic potential energy in the elastic element, equation (1) can be obtained according to the law of conservation of energy, where P represents the power when the hip joint performs negative work, t represents the corresponding time when the hip joint performs negative work, and k is the optimal stiffness of the exoskeleton hip joint, θ is the joint rotation angle.

$$W = \int P dt = \frac{1}{2} k\theta^2 \tag{1}$$

In this study, a seven-link dynamic model of the human body is established by the Lagrange method to solve the torque of the hip joint, as shown in Fig. 5. It is assumed that the mass of each connecting rod is concentrated in the center of the connecting rod, and θ_i (i = 1, 2, 3,..., 7) is the relative angle between the connecting rod and the vertical line of the ground. The human walking process is composed of the monopedal support phase and the bipedal support phase. The bipedal support phase accounts for a small proportion of the whole gait cycle, so the bipedal support phase is ignored here. Taking the tip of the left foot of the model in Fig. 5 as the origin, the sagittal axis as the X-axis, and the vertical axis as the Z-axis the coordinates (x_i, z_i) (i = 1, 2, 3, ..., 7) of the centroid position of each connecting rod can be obtained through the geometric relationship:

$$\begin{cases} x_i = a_i \sin\theta_i + \sum_{j=1}^{i-1} A_j l_j \sin\theta_j \\ z_i = a_i \cos\theta_i + \sum_{j=1}^{i-1} A_j l_j \cos\theta_j \end{cases} \quad A_j = \begin{cases} 0j=4 \\ 1j=1,2,3,5,6,7 \end{cases} \tag{2}$$

From (2), it can be found that the kinetic energy E_k and potential energy E_p of the system are

$$E_k = \sum_{i=1}^{7} \frac{1}{2} m_i (\dot{x}_i^2 + \dot{y}_i^2) + \frac{1}{2} I_i \dot{\theta}_i^2 = \frac{1}{2} \dot{\theta}^T J \dot{\theta} \tag{3}$$

and

$$E_p = \sum_{i=1}^{7} m_i g z_i = \sum_{i=1}^{7} N_i g \cos\theta_i \tag{4}$$

In (2) – (4), a_i, l_i, m_i, and I_i (i = 1, 2, 3, ..., 7) are the center distance, connecting rod length, connecting rod mass, and moment of inertia of each connecting rod, respectively. J is the mass inertia matrix, g is the gravity constant, and N_i is expressed as follows:

$$\begin{cases} N_i = m_i a_i + \sum_{j=i+1}^{7} m_j l_i & i = 1, 2, 3 \\ N_i = m_i a_i & i = 4, 7 \\ N_i = m_i (l_i - a_i) + \sum_{j=i+1}^{7} m_j l_i & i = 5, 6 \end{cases} \tag{5}$$

By introducing (2) – (5) into the Lagrange equation, the dynamic expression of the human lower limb model in the monopedal support phase is

$$A(\theta)\ddot{\theta} + \mathrm{B}(\theta, \dot{\theta})\dot{\theta} + C(\theta) = \tau, \tag{6}$$

where τ is the hip joint torque, A is the inertia matrix, B is the first-order differential matrix, which is related to the centripetal force and Coriolis force, and C is the matrix related to gravity:

$$\begin{aligned} A(\theta) &= J(\theta) = [L_{ij} \cos(\theta_i - \theta_j)]_{7\times7} \\ B(\theta, \dot{\theta}) &= [L_{ij} \sin(\theta_i - \theta_j)\dot{\theta}_j]_{7\times7} \\ C(\theta) &= [N_i g \cos\theta_i]_{7\times1} \end{aligned} \tag{7}$$

$$L_{ij} = \begin{cases} L_{ji} & j < i \\ I_i + m_i a_i^2 + A_i (\sum_{k=j+1}^{6} m_k) l_i^2 & j = i \\ A_i l_i m_j a_j + A_i A_j (\sum_{k=j+1}^{6} m_k) l_i l_j & j > i \end{cases} \tag{8}$$

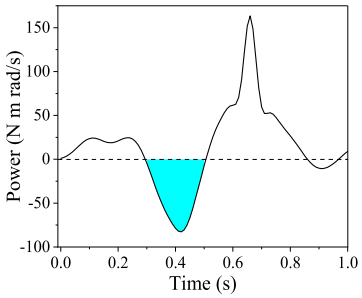

Fig. 6. Changes of the hip joint power in a single gait cycle.

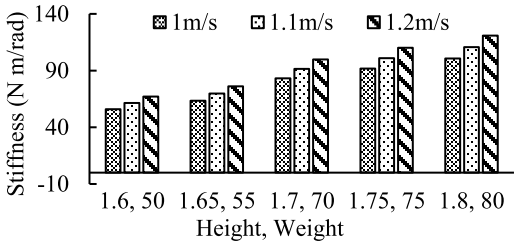

Fig. 7. Optimized stiffness at different walking speeds for different heights and weights.

TABLE I
TECHNICAL INDEX OF VS-ESAH EXOSKELETON

INDEX	Value
VS joint rotation angle	−0.35–0.35 rad
Torque	17.5–49 N m
Stiffness adjustment range	50–120 N m/rad

After the torque τ of the hip joint is obtained according to the above dynamic equation, combined with the angle θ of the hip joint, the hip joint power shown in Fig. 6 can be obtained. Then, according to (1), the energy that can be stored in the elastic element is obtained by integrating the negative work area of the hip joint (the blue area in Fig. 6), and finally the optimal stiffness K of the VS joint can be calculated.

Using this optimization method, the optimal assist stiffness of five people with different height and weight under three different walking speeds is obtained. As can be seen from Fig. 7, with the increase of height and weight, the optimized assist stiffness of different people gradually increases. For the same person, with the increase of speed, the optimal assist stiffness also gradually increases. The optimal assist stiffness for a person with height of 1.6 m, weight of 50 kg, and walking speed of 1 m/s is 55 N m/rad, and that of a person with height of 1.8 m, weight of 80 kg, and speed of 1 m/s is about 120 N m/rad.

Based on the previous analysis, the design indexes for VS-ESAH exoskeleton are shown in Table I. These indexes can cover the population of 1.6–1.8 m height and 50–80 kg weight.

IV. DESIGN OF VS-ESAH EXOSKELETON

The cam roller VS mechanism realizes stiffness adjustment by using the characteristics of the change of the curvature radius in the process of cam rotation. Compared with other mechanisms, it has a compact structure and can effectively reduce the weight of the mechanism. Therefore, the cam roller mechanism is adopted in this study.

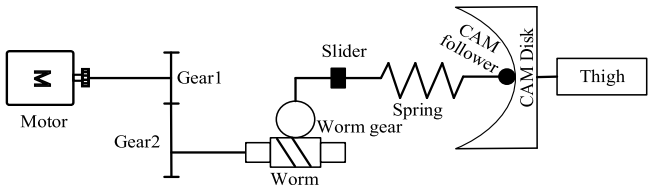

Fig. 8. Working principle of the VS joint.

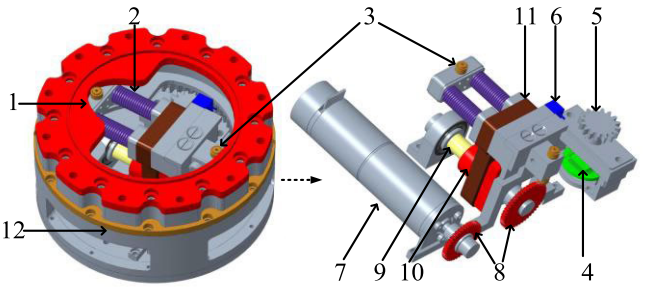

Fig. 9. VS joint structure design diagram of VS-ESAH exoskeleton.

Fig. 8 shows the principle of the cam VS joint mechanism designed in this study. The mechanism mainly includes a motor, gear set, worm, spring, guide rod, slider, roller, and cam. The rotation of the motor is transmitted to the slider through the gear and worm, and the slider pushes the spring along the guide rod to compress and achieve stiffness adjustment. The worm mechanism in the VS module has the ability of one-way transmission, which can avoid the reverse push of the roller to the spring when the roller bears load.

Fig. 9 shows the three-dimensional model of the VS hip joint designed in this study. To reduce the local stress of the joint, two groups of springs are set in the mechanism, and a guide rod is inserted in the middle of the spring. An absolute position sensor is used to measure the rotation angle of the hip joint.

In the design of the vs joint, the motor is only used to adjust the compression of the spring to achieve changes in the stiffness of the exoskeleton joint without directly providing auxiliary torque. And the motor only works when the exoskeleton stiffness needs to be adjusted, so its power consumption is very small. The specially designed cam disk will move relative to the cam disk follower when walking, so as to compress the spring and store most of the negative work done by the hip joint in the elastic element to assist walking. For the entire VS-ESAH exoskeleton, it still uses the energy storage and assistance principle of passive exoskeleton, so we still define it as passive exoskeleton or quasi passive exoskeleton.

Through the analysis of gait and joint power of lower limbs, the exoskeleton can compress the internal spring to store the negative work done by the human body from the mid stance to the terminal stance of the support phase, and

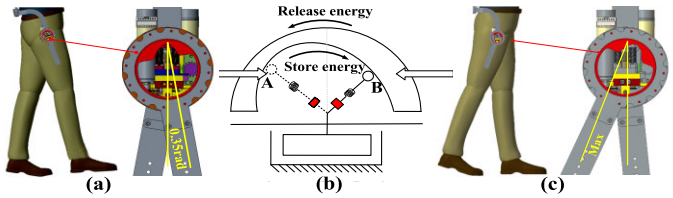

Fig. 10. Schematic diagram of energy storage and assistance of VS-ESAH exoskeleton. (a) Start position of energy storage (b) Stiffness regulation motor (c) End position of energy storage.

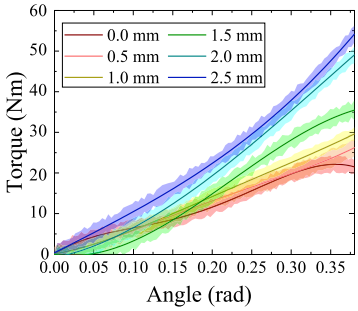

Fig. 11. Static stiffness test of the VS joint.

then release the energy stored by the spring to help the thigh move forward in the swing phase. At the beginning of energy storage, the position of the hip joint is at about 0.35 rad in a flexion position, and at the end of energy storage, the hip joint is in the maximum extension position. After that, the energy is released from the maximum extension position to achieve flexion assistance. As shown in Fig. 10(a), when the hip joint is in flexion at 0.35 rad, the roller is located at point A shown in Fig. 10(b). As shown in Fig. 10(c), the hip joint is in the maximum extension position, and the roller is located at point B of Fig. 10(b). When the hip joint moves from Fig. 10(a) to (c), the roller moves from point A to point B, and the spring is compressed to store energy. When the hip joint moves from Fig. 10(c) to (a), the roller moves from point B to point A, and the energy stored in spring is released. The cam contour between point A and point B in Fig. 10(b) is in the shape of an ellipse.

Then the static stiffness of VS joint is measured. The measurement process is as follows. The torque required to rotate VS joint at different angles is recorded with different spring compression. The results are shown in Fig. 11. It can be seen from the figure that with the increase of spring compression amount, the stiffness value gradually increases at the same rotation angle, but with the same compression amount, the stiffness value of the VS joint can be approximately constant. When the spring compression is 0.5 mm, 1 mm, 2 mm, and 2.5 mm, the equivalent stiffness of the joint is approximately 62.04 N m/rad, 70.11 N m/rad, 116.19 N m/rad, and 128.28 N m/rad, respectively, which is within the stiffness adjustment range in Table I.

V. Assistance Performance Experiments

A. Experimental Scheme Design

The purpose of this experiment is to evaluate the assistance effect of the VS-ESAH exoskeleton. Considering that the main application scenario of the exoskeleton is walking assistance, and the assistance effect of exoskeleton can be reflected through muscle fatigue. Studies have shown that endurance tasks are more likely to cause muscle fatigue [32]. Therefore, this paper intends to reflect the assistance effect of exoskeleton through the long-time walking experiment on treadmill and the analysis of muscle fatigue.

Muscle fatigue is defined as the decrease of muscle contractility after long-term exercise. At present, muscle fatigue can be assessed by subjective perception, mechanical indicators, biochemical indicators, and electromyography (sEMG) signals. The way of quantifying subjective fatigue through the Rating of Perceived Exercise (RPE) is greatly affected by individual differences. The measurement of mechanical indexes such as the Maximal Voluntary Contraction (MVC) of muscle requires additional professional equipment. The collection of biochemical indicators such as blood lactic acid is invasive. Considering that the electromyography (sEMG) sensor is portable and non-invasive, and can record data throughout the experiment, the surface electromyography signal is used to evaluate muscle fatigue [33].

While walking on flat ground, the main driving muscles of hip flexion and extension are the rectus femoris (RF) and long head of the biceps femoris (BF). Therefore, muscle fatigue is judged by measuring sEMG signals of the rectus femoris and long head of the biceps femoris during walking.

Since the sEMG signal measured during walking is periodic and the period is relatively short, it is necessary to obtain long-term data from sEMG signals to evaluate muscle fatigue. The amount of data obtained from long-term sampling is huge, and the trend cannot be seen directly from the data. Therefore, the data should be processed to extract the eigenvalues of sEMG signals from the data, and reflect the muscle fatigue status through the eigenvalues. In this paper, time-domain and frequency-domain indicators are selected to evaluate muscle fatigue and reflect the assistance effect of exoskeleton. The root mean square (RMS) is selected for the time domain, and the median frequency (MF) and mean power frequency (MPF) are analyzed in the frequency domain. Among them, RMS can reflect the change of sEMG signal amplitude caused by muscle fatigue, while MF and MPF can well reflect the change of sEMG signal frequency caused by muscle fatigue. When muscle fatigue occurs, RMS will increase, while MF and MPF will decrease.

Five subjects are recruited, with an average age of 24 ± 2 years. Two subjects are women with heights of 1.6 m and 1.65 m and masses of 50 kg and 55 kg, and three subjects are men with heights of 1.7 m, 1.75 m, and 1.8 m and masses of 70 kg, 75 kg, and 80 kg. Walking condition variables are limited to walking speed, which is set as 1 m/s, 1.1 m/s, and 1.2 m/s. All subjects participated in the experiment in a good resting state, and did not eat any alcoholic food or use any drugs within 24 hours before the experiment.

Fig. 12 shows the optimized exoskeleton stiffness of different subjects under different walking conditions and the spring pre compression required to achieve the optimal stiffness. The bar graph represents the optimal stiffness corresponding to

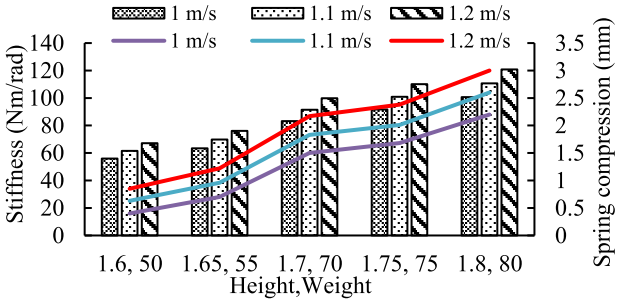

Fig. 12. Optimized stiffness and spring compression for different subjects.

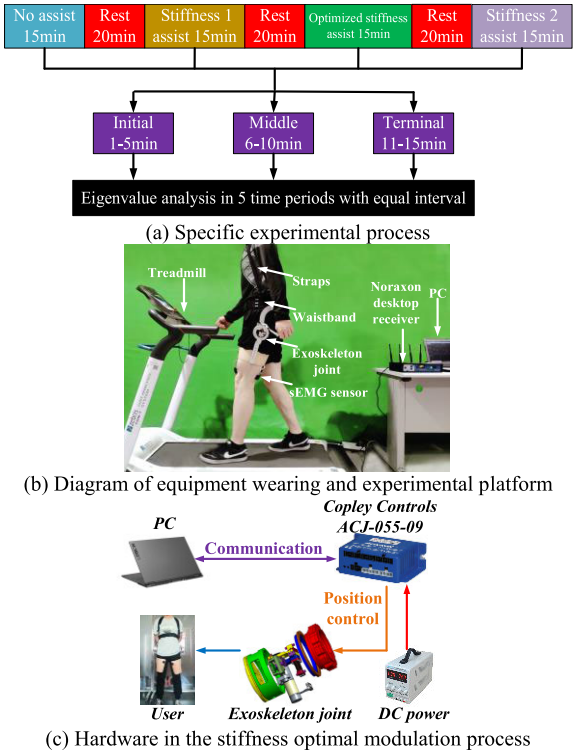

Fig. 13. Assistance performance experiments scheme.

different walking speeds of the subjects, while the line graph represents the corresponding spring pre compression.

Finally, in order to verify that the optimized stiffness can minimize the energy consumption in the walking process, it is also necessary to set two groups of other stiffness values randomly for the same conditions, and compare the muscle fatigue under different stiffness values.

The specific experimental scheme is shown in Fig. 13(a). Firstly, the subjects wore exoskeletons and sEMG signal acquisition devices as shown in Fig. 13(b), and walked on the treadmill for 15 minutes. At this time, the exoskeleton is in the state of no assistance, and then the subjects rest for 20 minutes. Secondly, the stiffness of exoskeleton is adjusted to stiffness 1, which is less than the optimized stiffness. The subjects walk for 15 minutes and then rest for 20 minutes. After that, the stiffness is adjusted to optimal stiffness. The subjects walk for 15 minutes and then rest for 20 minutes. Finally, the stiffness is adjusted to stiffness 2, which is greater than the optimized stiffness, and the subjects walk for 15 minutes.

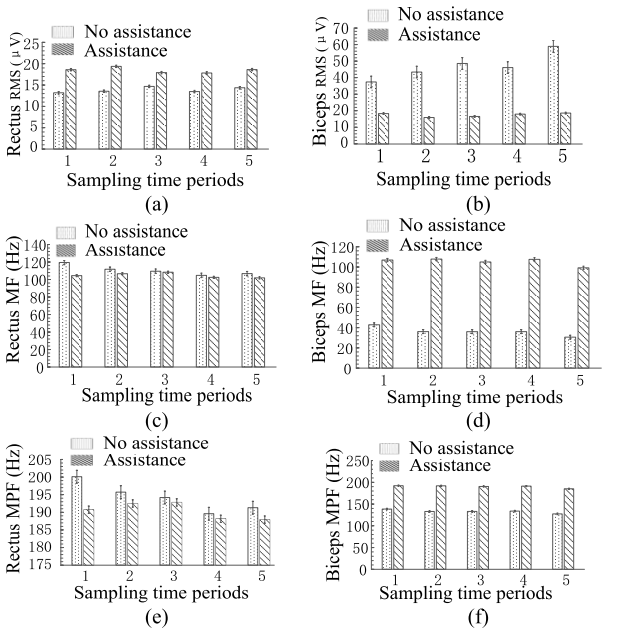

Fig. 14. Eigenvalues of five sampling time periods extracted equidistantly from the 1-5minute time period of two muscles.

Fig. 13(c) shows our hardware system in detail. In the current scheme, we do not integrate the controller, driver and battery into the exoskeleton, and the exoskeleton weighs 3.32kg. And the whole stiffness optimization process is realized offline. Firstly, according to the wearer's height, weight and walking speed, the optimal stiffness and the corresponding spring compression amount are calculated on the PC using the stiffness optimization method. Then, when the exoskeleton is not in use, the PC running software sends instructions to the driver to control the stiffness adjustment motor, and then adjusts the stiffness of exoskeleton. In this process, we used EC-MAX22-GP22C servo motor of maxon company as the stiffness adjusting motor in the exoskeleton, and ACJ-055-18 micro driver of Copley Controls company as the driver. During the experiment, the treadmill used was the Zebris FDM-T gait analysis treadmill, and the sEMG acquisition device used was the Noraxon Ultium sEMG acquisition system, with a sampling frequency of 1500Hz.

B. Experimental Results and Data Processing

In the eigenvalues diagrams (the eigenvalues diagrams of one subject under different conditions is shown as an example in Supplementary fig. 1 in the Appendix), the power-frequency diagram only shows the change trend, which is not enough to draw a definite conclusion on the assistance effect of the VS-ESAH exoskeleton. Therefore, it is necessary to use the eigenvalues (RMS, MF, MPF) of sEMG signals for qualitative and quantitative analysis.

Here, the data of a subject is taken as an example to introduce the processing of eigenvalue data. Firstly, five sampling time periods of the same size are extracted from each interval of three kinds of eigenvalues data at an equal distance, and each sampling time period includes the same number of sampling points. The average value of each sampling time period is

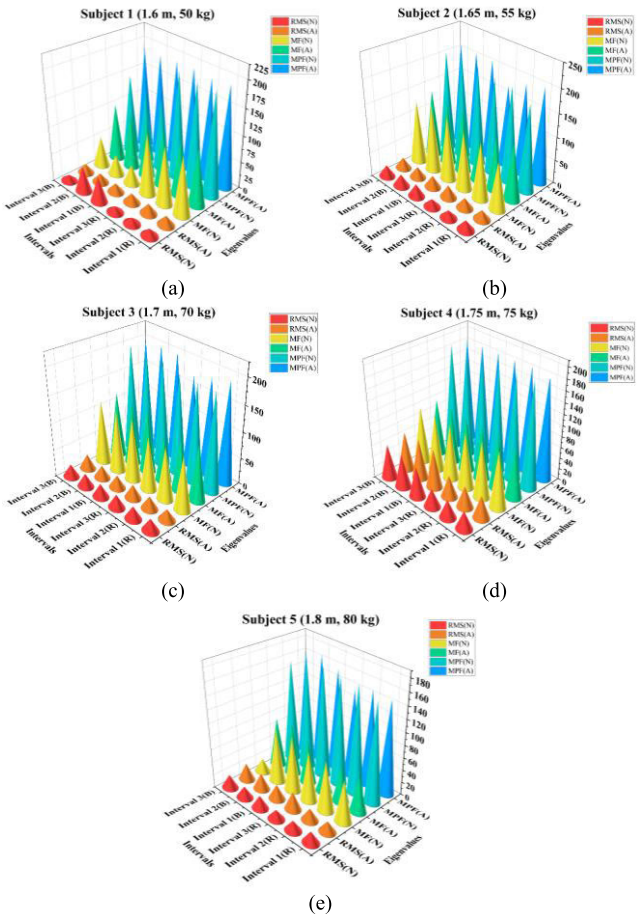

Fig. 15. The average eigenvalues of five sampling time periods of five subjects in each time interval.

calculated, and then they are compared and analyzed. The data in Fig. 14 shows the eigenvalues of five sampling time periods extracted equidistantly from the 1-5minute time period of the two muscles. (See the Supplementary fig. 2 and Supplementary fig. 3 in the Appendix for the average eigenvalues of 6–15 min). The data of five subjects were processed as above, and the results are summarized in Fig. 15. In the figure, N represents no assistance, A represents assistance. R represents RF, and B represents BF. Each subject's 15 min walk is divided into three intervals, where interval 1 is from 1–5 min, interval 2 is from 6–10 min, and interval 3 is from 11–15 min. The average RMS, average MF and average MPF of five sampling time periods of five subjects in each time interval are shown in Fig. 15(b)–(d) respectively.

In order to show the assistance effect under different stiffness more specifically, the eigenvalue MF of five subjects under different stiffness was directly analyzed quantitatively. Fig. 16 shows the eigenvalue MF of five subjects under three kinds of assist stiffness. Stiffness 1 and stiffness 2 are randomly set, one of which is greater than the optimal stiffness and the other is less than the optimal stiffness.

C. Experimental Results Analysis

According to the data in the Fig. 15 and the histogram in each of the five sampling time periods, for the subject 1 with

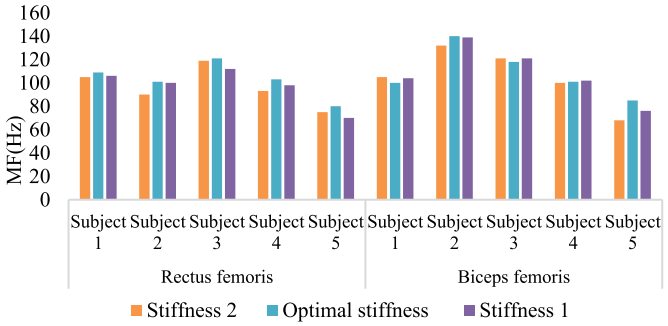

Fig. 16. Eigenvalue MF of five subjects with the assistance of optimal stiffness and random stiffness.

a height of 1.6 m and mass of 50 kg, in interval 1, the RMS of RF decreases, while the MF and MPF both increase, and the RMS of the long head of BF increases, while the MF and MPF both decrease, indicating that fatigue of RF decreased and fatigue of BF increased. In interval 2, except that the RMS of the long head of BF decreases, the other trends are the same as those in interval 1, indicating that fatigue of RF decreased. In interval 3, the change trends of the three eigenvalues of RF are consistent with those in intervals 1 and 2, indicating that fatigue of RF decreased, while the three eigenvalues of the BF all increase. As a whole, the fatigue degree of RF of subject 1 decreased, while the fatigue degree of BF increased. Other subjects are analyzed in the same way.

For subject 2 with a height of 1.65 m and mass of 55 kg, in interval 1, RMS of RF decreased, while MF and MPF increased, indicating that fatigue of RF decreased, and RMS of BF did not change significantly, while MF and MPF decreased. In interval 2, RMS of RF increased, while MF and MPF decreased, and the three eigenvalues of BF decreased, indicating that the fatigue of RF increased. In interval 3, the change trend of the eigenvalues of RF was consistent with that in interval 2. The increase of MF and MPF of BF showed that the fatigue of RF increased. From the overall perspective of the three intervals, the fatigue degree of subject 2 decreased in the early stage of the experiment, but increased in the middle and late stages.

For the subject 3 with a height of 1.7 m and mass of 70 kg, in interval 1, RMS of RF decreased, while MF and MPF increased, indicating that the fatigue of RF decreased, and the eigenvalues of BF did not change significantly. In interval 2, the eigenvalues of RF and BF did not change significantly. In interval 3, the MF and MPF of RF decreased, indicating that the fatigue of RF decreased, and the eigenvalues of BF did not change significantly. As a whole, the fatigue degree of RF muscle of subject 3 decreased in the experiment.

For the subject 4 with a height of 1.75 m and mass of 75 kg, the RMS of the RF decreases, while the MF and MPF both increase, indicating that fatigue of RF decreased, and the changes of the eigenvalues of BF are irregular.

For the subject 5 with a height of 1.8 m and mass of 80 kg, in interval 1, the RMS of RF did not change significantly, while MF and MPF increased, and the RMS of BF increased, while MF and MPF decreased, indicating that the fatigue of BF increased. In interval 2, RMS of RF and BF decreased, while

MF and MPF increased, indicating that fatigue of both muscles decreased. At interval 3, RMS of RF decreased, while MF and MPF increased, and the three eigenvalues of BF increased, indicating that the fatigue degree of RF decreased. As a whole, the fatigue of RF decreased and the fatigue of BF increased.

In the qualitative analysis of no assist and optimal stiffness assist experiments, it can be seen that wearing of exoskeleton can reduce the muscle fatigue of RF to a certain extent. For the long head of BF, the fatigue degree of some subjects showed an upward trend, and the fatigue change of others was uncertain.

In order to make the assistance effect more specific, the data will be comprehensively analyzed quantitatively. It is generally believed that frequency domain indicators have good performance in evaluating muscle fatigue, and MF is less affected by noise, while RMS is often used as an assistance evaluation standard [34]. Therefore, we use MF as the evaluation index to analyze the data of five subjects under random stiffness and optimal stiffness in Fig. 16.

For subject 1, with the assistance of stiffness 1, optimal stiffness, and stiffness 2, the fatigue degree of RF decreased by 8.4%, 13.9%, 2.9% respectively, while the fatigue degree of long head of BF increased by 2.1%, 1.4%, and 7.0% respectively. When subject 1 was assisted by the optimal stiffness, the effect of exoskeleton on reducing the fatigue of two muscles was better than that of two random stiffness.

For subject 2, with the assistance of stiffness 1, optimal stiffness, and stiffness 2, the fatigue degree of RF increased by 2.5%, 1.6%, 12.2% respectively, while the fatigue degree of BF increased by 0.9%, 1.9%, 0.9% respectively. When subject 2 was assisted by the optimal stiffness, the effect of exoskeleton on reducing the fatigue degree of RF was better than that of random stiffness, and the effect on reducing the fatigue degree of BF was worse than that of random stiffness.

For subject 3, with the assistance of stiffness 1, optimal stiffness, and stiffness 2, the fatigue degree of RF decreased by 5.9%, 8.9%, and 4.9% respectively, while the fatigue degree of BF increased by 0.8%, 2.4%, and 4.1% respectively. When subject 3 was assisted by the optimal stiffness, the effect of exoskeleton on reducing the fatigue degree of RF was better than that of random stiffness, and the effect on reducing the fatigue degree of BF was between two random stiffness.

For subject 4, with the assistance of stiffness 1, optimal stiffness, and stiffness 2, the fatigue of RF increased by 0.8%, decreased by 11%, and decreased by 5.3% respectively, while the fatigue of BF decreased by 0.5%, 2.0%, and increased by 1.1% respectively. When subject 4 was assisted by the optimal stiffness, the effect of exoskeleton on reducing the fatigue of two muscles was better than that of two random stiffness.

For subject 5, with the assistance of stiffness 1, optimal stiffness, and stiffness 2, the fatigue degree of RF decreased by 2.6%, decreased by 9.7%, and increased by 4.25%, while the muscle fatigue of BF increased by 14.4%, 5.56%, and 19.1% respectively. When subject 5 was assisted by the optimal stiffness, the effect of exoskeleton on reducing the fatigue of two muscles was better than that of two random stiffness.

TABLE II
SUMMARY OF QUALITATIVE AND QUANTITATIVE ANALYSIS OF EXPERIMENTAL RESULTS

Subject	Muscle	Qualitative analysis	Quantitative analysis
Subject 1	RF	Decreased	-13.9%
1.6m, 50kg	BF	Increased	+1.4%
Subject2	RF	Decreased at first	+1.6%
1.65m, 55kg	BF	Increased	+1.9%
Subject 3	RF	Decreased	-8.9%
1.7m, 70kg	BF	uncertain	+2.4%
Subject 4	RF	Decreased	-11.0%
1.75m, 75kg	BF	uncertain	-2.0%
Subject 5	RF	Decreased	-9.7%
1.8m, 80kg	BF	Increased	+5.56%

This table summarizes the qualitative and quantitative analysis of the experimental results in Section V.C. The qualitative analysis described the changes of RF and BF muscle fatigue after being assisted by exoskeleton. The quantitative analysis is the change of RF and BF fatigue degree under the optimal stiffness, where "+" indicates the increase of fatigue degree and "-" indicates the decrease of fatigue degree.

Based on the above analysis, the qualitative and quantitative analysis of results are summarized in TABLE II.

In the assistance experiments with different stiffness, it can be seen that under the optimal stiffness, the fatigue degree of RF of the other four subjects decreased to a certain extent except that of subject 2 increased, and the fatigue degree of RF of the other four subjects increased to a certain extent except that of subject 4 decreased. At the same time, under the optimal stiffness, for five subjects, the reduction of fatigue degree of RF by exoskeleton was better than two random stiffness, and for subjects 1, 4 and 5, the increase of fatigue degree of BF by exoskeleton was less than two random stiffness.

According to the relationship between the eigenvalues of sEMG signal and muscle fatigue, the fatigue of RF decreased by an average of 8.5% compared with that without assistance, but the fatigue of the long head of BF increased slightly, with an average increase of about 1.8%.

VI. DISCUSSIONS

According to the kinematic function of the lower limb skeletal muscle, RF is dominated by the femoral nerve, the long head of the BF is dominated by the sciatic nerve. Both of them play an important role in the flexion and extension of the hip joint. The VS-ESAH exoskeleton designed in this study can reduce muscle fatigue of RF, assist hip flexion, and perform best under the optimal stiffness. In addition, according to the experimental data, exoskeleton either has no significant effect on the long head of BF, or slightly increases the muscle burden.

In the experimental analysis of sEMG signals, we finally took MF as the standard for quantitative analysis. At the same time, we found that RMS has a small difference with MF in the reflection of muscle fatigue trend. It is likely that RMS mainly reflects the amplitude of sEMG signals, and the change of amplitude is more likely to be affected by external factors [35].

By comparing with the work of other researchers, we also get a lot of inspiration. Chen et al. developed peEXO [36] hip joint exoskeleton, and found that small stiffness has a small assistant effect on walking, while excessive stiffness will significantly increase the metabolic energy cost of walking. This conclusion is consistent with our experimental results obtained by comparing the random stiffness with the optimal stiffness.

The exoskeleton designed by Nasiri et al. can reduce the metabolic cost by about 6%∼8%, and its weight is 1.3 kg [12]. The weight of his device is only about half of that of VS-ESAH exoskeleton, but it is close to the assistance effect of this study. It can be seen that how to optimize the weight of the equipment is a very urgent task for this study. However, the change of its stiffness is achieved by replacing the elastic elements. At this point, our design is more convenient.

The passive exoskeleton of hip and knee joints designed by Zhou et al. can reduce the metabolic cost of the wearer by up to 10.1%, which is superior to the 8.6% assistance effect of VS-ESAH exoskeleton [37]. Its multi joint design is more ingenious, which fully considers the cooperative movement between the hip joint and the knee joint. This is very reasonable, because walking is originally a multi joint movement of the lower limbs. Considering the energy flow between the multi joints, a more reasonable assistance strategy may be developed. In addition, its clutch design also avoids the extra load on BF. These provide us with inspiration for further research.

Furthermore, there are obvious areas for improvement in this study. Firstly, because the cam contour in this study adopts an elliptic shape, the stiffness in Fig. 11 is only approximately linear. In our subsequent work, the VS joint will be optimized so that the stiffness of the joint is only related to the compression of the spring. Secondly, the stiffness is adjusted after off-line calculation in this study, but a real-time on-line adjustment method for VS joints will need to be developed in subsequent research. Meanwhile the energy storage range of hip exoskeleton is set to range from −0.35rad to 0.35rad, which is an average based on data from most people, but may not be accurate for everyone. In addition, only five subjects were recruited in this study. Although the experimental data show that exoskeleton has a certain assistance effect, the universality of this conclusion is not strong enough because the subject population is not large enough. In the subsequent research, we will also consider expanding the subject population to more accurately reflect the impact of exoskeleton.

VII. Conclusion

Based on the analysis of the energy flow characteristics of lower limb joints and the equivalent stiffness of the hip joint while walking on flat ground, an energy storage assisted hip exoskeleton based on a cam roller VS mechanism is designed in this study. The exoskeleton can store the negative work done by the hip joint, assist in the swing period, and have the ability to adjust the stiffness to adapt to the optimal stiffness changes of different height and weight wearers at different speeds. By establishing a seven link human dynamics model, the optimal stiffness of the exoskeleton is finally obtained with the objective of fully storing the negative work of the hip joint from the middle to the end of standing. Finally, a muscle fatigue experiment is designed to verify the assistance effect of the exoskeleton. The sEMG signals of RF and BF are measured and the eigenvalues are analyzed. Taking MF as the evaluation index, it is found that the exoskeleton can significantly reduce the muscle fatigue of RF, while walking on flat ground, and the assistance effect is more obvious under the optimal stiffness, but the assistance effect for BF is not significant.

Appendix

A figure titled “Supplementary Fig. 1” is add to this paper, presenting the eigenvalues diagrams of one subject under the conditions of no assistance and optimal stiffness assistance.

Two figures titled “Supplementary Fig. 2” and “Supplementary Fig. 3” are add to this paper, presenting the average eigenvalues of 6–15 min.

References

[1] B. Zhang, T. Liu, B. Zhang, and M. G. Pecht, “Recent development of unpowered exoskeletons for lower extremity: A survey,” *IEEE Access*, vol. 9, pp. 138042–138056, 2021.

[2] R. Bogue, “Exoskeletons and robotic prosthetics: A review of recent developments,” *Ind. Robot, Int. J.*, vol. 36, no. 5, pp. 421–427, 2009.

[3] A. B. Zoss, H. Kazerooni, and A. Chu, “Biomechanical design of the Berkeley lower extremity exoskeleton (BLEEX),” *IEEE/ASME Trans. Mechatronics*, vol. 11, no. 2, pp. 128–138, Apr. 2006.

[4] A. Tsukahara, Y. Hasegawa, K. Eguchi, and Y. Sankai, “Restoration of gait for spinal cord injury patients using HAL with intention estimator for preferable swing speed,” *IEEE Trans. Neural Syst. Rehabil. Eng.*, vol. 23, no. 2, pp. 308–318, Mar. 2015.

[5] N.-S. Kwak, K.-R. M´uller, and S.-W. Lee, “Toward exoskeleton control based on steady state visual evoked potentials,” in *Proc. Int. Winter Workshop Brain-Comput. Interface (BCI)*, Feb. 2014, pp. 1–2.

[6] F. Zhu et al., “Effects of an exoskeleton-assisted gait training on post-stroke lower-limb muscle coordination,” *J. Neural Eng.*, vol. 18, no. 4, Aug. 2021, Art. no. 046039.

[7] Z. Lovrenovic and M. Doumit, “Development and testing of a passive walking assist exoskeleton,” *Biocybernetics Biomed. Eng.*, vol. 39, no. 4, pp. 992–1004, Oct. 2019.

[8] S. H. Collins, M. B. Wiggin, and G. S. Sawicki, “Reducing the energy cost of human walking using an unpowered exoskeleton,” *Nature*, vol. 522, no. 7555, p. 212, 2015.

[9] L. M. Mooney and H. M. Herr, “Biomechanical walking mechanisms underlying the metabolic reduction caused by an autonomous exoskeleton,” *J. NeuroEng. Rehabil.*, vol. 13, no. 1, pp. 1–12, Jan. 2016.

[10] D. J. Farris and G. S. Sawicki, “The mechanics and energetics of human walking and running: A joint level perspective,” *J. Roy. Soc. Interface*, vol. 9, no. 66, pp. 110–118, Jan. 2012.

[11] T. Zhou, C. Xiong, J. Zhang, D. Hu, W. Chen, and X. Huang, “Reducing the metabolic energy of walking and running using an unpowered hip exoskeleton,” *J. NeuroEng. Rehabil.*, vol. 18, no. 1, pp. 1–15, Jun. 2021.

[12] R. Nasiri, A. Ahmadi, and M. N. Ahmadabadi, “Reducing the energy cost of human running using an unpowered exoskeleton,” *IEEE Trans. Neural Syst. Rehabil. Eng.*, vol. 26, no. 10, pp. 2026–2032, Oct. 2018.

[13] M. M. Alemi, J. Geissinger, A. A. Simon, S. E. Chang, and A. T. Asbeck, “A passive exoskeleton reduces peak and mean EMG during symmetric and asymmetric lifting,” *J. Electromyogr. Kinesiol.*, vol. 47, pp. 25–34, Aug. 2019.

[14] Y. Ding, M. Kim, S. Kuindersma, and C. J. Walsh, “Human-in-the-loop optimization of hip assistance with a soft exosuit during walking,” *Sci. Robot.*, vol. 3, no. 15, Feb. 2018, Art. no. eaar5438.

[15] B. Zhong, K. Guo, H. Yu, and M. Zhang, “Toward gait symmetry enhancement via a cable-driven exoskeleton powered by series elastic actuators,” *IEEE Robot. Autom. Lett.*, vol. 7, no. 2, pp. 786–793, Apr. 2022.

[16] M. Okui, S. Iikawa, Y. Yamada, and T. Nakamura, "Variable viscoelastic joint system and its application to exoskeleton," in *Proc. IEEE/RSJ Int. Conf. Intell. Robots Syst. (IROS)*, Sep. 2017, pp. 3897–3902.

[17] J. Zhang, M. Cong, D. Liu, Y. Du, and H. Ma, "A lightweight variable stiffness knee exoskeleton driven by shape memory alloy," *Ind. Robot, Int. J. Robot. Res. Appl.*, vol. 49, no. 5, pp. 994–1007, Jun. 2022.

[18] W. Cao et al., "A lower limb exoskeleton with rigid and soft structure for loaded walking assistance," *IEEE Robot. Autom. Lett.*, vol. 7, no. 1, pp. 454–461, Jan. 2022.

[19] J. Sun, Z. Guo, D. Sun, S. He, and X. Xiao, "Design, modeling and control of a novel compact, energy-efficient, and rotational serial variable stiffness actuator (SVSA-II)," *Mechanism Mach. Theory*, vol. 130, pp. 123–136, Dec. 2018.

[20] Z. Li, S. Bai, O. Madsen, W. Chen, and J. Zhang, "Design, modeling and testing of a compact variable stiffness mechanism for exoskeletons," *Mechanism Mach. Theory*, vol. 151, Sep. 2020, Art. no. 103905.

[21] O. Baser and H. Kizilhan, "Mechanical design and preliminary tests of VS-AnkleExo," *J. Brazilian Soc. Mech. Sci. Eng.*, vol. 40, no. 9, pp. 1–16, Sep. 2018.

[22] S. Kumar, M. R. Zwall, E. A. Bolívar-Nieto, R. D. Gregg, and N. Gans, "Extremum seeking control for stiffness auto-tuning of a quasi-passive ankle exoskeleton," *IEEE Robot. Autom. Lett.*, vol. 5, no. 3, pp. 4604–4611, Jul. 2020.

[23] M. Cestari, D. Sanz-Merodio, J. C. Arevalo, and E. Garcia, "An adjustable compliant joint for lower-limb exoskeletons," *IEEE/ASME Trans. Mechatronics*, vol. 20, no. 2, pp. 889–898, Apr. 2015.

[24] M. K. MacLean and D. P. Ferris, "Energetics of walking with a robotic knee exoskeleton," *J. Appl. Biomech.*, vol. 35, no. 5, pp. 320–326, Oct. 2019.

[25] X. Wu, W. Cao, H. Yu, Z. Zhang, Y. Leng, and M. Zhang, "Generating electricity during locomotion modes dominated by negative work via a knee energy-harvesting exoskeleton," *IEEE/ASME Trans. Mechatronics*, vol. 27, no. 6, pp. 4451–4461, Dec. 2022.

[26] G. Bovi, M. Rabuffetti, P. Mazzoleni, and M. Ferrarin, "A multiple-task gait analysis approach: Kinematic, kinetic and EMG reference data for healthy young and adult subjects," *Gait Posture*, vol. 33, no. 1, pp. 6–13, 2011.

[27] S. Galle, W. Derave, F. Bossuyt, P. Calders, P. Malcolm, and D. D. Clercq, "Exoskeleton plantarflexion assistance for elderly," *Gait Posture*, vol. 52, pp. 183–188, Feb. 2017.

[28] F. A. Panizzolo, C. Bolgiani, L. D. Liddo, E. Annese, and G. Marcolin, "Reducing the energy cost of walking in older adults using a passive hip flexion device," *J. NeuroEng. Rehabil.*, vol. 16, no. 1, pp. 1–9, Oct. 2019.

[29] G. S. Sawicki, C. L. Lewis, and D. P. Ferris, "It pays to have a spring in your step," *Exercise Sport Sci. Rev.*, vol. 37, no. 3, pp. 130–138, Jul. 2009.

[30] M. G. Browne and J. R. Franz, "More push from your push-off: Joint-level modifications to modulate propulsive forces in old age," *PLoS ONE*, vol. 13, no. 8, Aug. 2018, Art. no. e0201407.

[31] K. Shamaei, G. S. Sawicki, and A. M. Dollar, "Estimation of quasi-stiffness of the human hip in the stance phase of walking," *PLoS ONE*, vol. 8, no. 12, Dec. 2013, Art. no. e81841.

[32] J. Zhu, C. Yi, B. Wei, C. Yang, Z. Ding, and F. Jiang, "The muscle fatigue's effects on the sEMG-based gait phase classification: An experimental study and a novel training strategy," *Appl. Sci.*, vol. 11, no. 9, p. 3821, Apr. 2021.

[33] S. Morrison et al., "Walking-induced fatigue leads to increased falls risk in older adults," *J. Amer. Med. Directors Assoc.*, vol. 17, no. 5, pp. 402–409, May 2016.

[34] I. Kyranou, S. Vijayakumar, and M. S. Erden, "Causes of performance degradation in non-invasive electromyographic pattern recognition in upper limb prostheses," *Frontiers Neurorobot.*, vol. 12, p. 58, Sep. 2018.

[35] H. A. Yousif et al., "Assessment of muscles fatigue based on surface EMG signals using machine learning and statistical approaches: A review," *IOP Conf. Ser., Mater. Sci. Eng.*, vol. 705, Nov. 2019, Art. no. 012010.

[36] W. Chen, S. Wu, T. Zhou, and C. Xiong, "On the biological mechanics and energetics of the hip joint muscle–tendon system assisted by passive hip exoskeleton," *Bioinspiration Biomimetics*, vol. 14, no. 1, Dec. 2018, Art. no. 016012.

[37] T. Zhou, C. Xiong, J. Zhang, W. Chen, and X. Huang, "Regulating metabolic energy among joints during human walking using a multiarticular unpowered exoskeleton," *IEEE Trans. Neural Syst. Rehabil. Eng.*, vol. 29, pp. 662–672, 2021.